Nonlinear Dyn (2017) 88:1373–1383
DOI 10.1007/s11071-016-3316-x

ORIGINAL PAPER

Two-dimensional localized Peregrine solution and breather excited in a variable-coefficient nonlinear Schrödinger equation with partial nonlocality

Chao-Qing Dai · Jiu Liu · Yan Fan · Ding-Guo Yu

Received: 30 October 2016 / Accepted: 21 December 2016 / Published online: 19 January 2017

Abstract Hierarchies of Peregrine solution and breather solution are derived in a (2+1)-dimensional variable-coefficient nonlinear Schrödinger equation with partial nonlocality. Based on these solutions, we study the control of the excitation of Peregrine solution and breather solution in different planes. In particular, the localized Peregrine solution and breather solution are firstly reported in two-dimensional space. It is expected that our analysis and results may give new insight into higher-dimensional localized rogue waves in nonlocal media.

Keywords Localized Peregrine solution and breather solution · Nonlinear Schrödinger equation · Partial nonlocality

1 Introduction

Localized structures based on different nonlinear evolution equations were intensively studied [1–6]. Peregrine solution and breather solution based on the nonlinear Schrödinger equation (NLSE) have become important prototypes to describe rogue wave motions in different fields of physics and ocean engineering [10–13]. Localized structures based on quintic and cubic-quintic NLSEs were extensively discussed [7–9]. Rogue waves are also called as freak waves, monster waves, killer waves. One of important characteristics of rogue waves is their unpredictability that “waves that appear from nowhere and disappear without a trace” [14].

In ocean, rogue waves exhibit harmful aspects, and they destroy ships and marine structures [15,16]. Many mainstream media such as Nature News, BBC News, Reuters, ScienceDaily, Physicsworld, Financial Express. have reported their extreme hazards in different sea areas. However, rogue waves can occur in other media than water. In particular, optical rogue waves allow study of the phenomenon in the laboratory. In optics, scientists excite rogue waves in the useful fields, e.g., harnessing and control of optical rogue waves in supercontinuum generation [17,18].

Relative to a reference frame co-moving with the optical pulse, the basic nonlinear model describing the rogue wave phenomenon is the focusing NLSE

$$iU_T + U_{XX} + 2|U|^2U = 0. \quad (1)$$

Based on this model, the theoretical study for rogue wave began with the pioneering work of Akhmediev’s group [14,19–22]. By means of the Darboux transformation, hierarchies of Peregrine solution and breather solution for NLSE have been reported to describe rogue waves [14,19–22].

Considering the concept of nonautonomous solitons [23], nonautonomous Peregrine solution and breather solution and the related control of excitation have

C.-Q. Dai (✉) · J. Liu · Y. Fan · D.-G. Yu
School of Sciences, Zhejiang A & F University,
Lin’an 311300, Zhejiang, People’s Republic of China
e-mail: dcq424@163.com

been discussed [24–26]. Moreover, nonautonomous Peregrine solution and breather solution in higher-dimensional case have also been studied [27–29]. However, all higher-dimensional Peregrine solution and breather structures in previous literatures [27–29] are not completely localized in space (such as x-y space).

In this paper, we consider the propagation of localized Peregrine solution and breather structures in a medium with partially nonlocal inhomogeneous nonlinearities by the following (2+1)-dimensional NLSE

$$\mathrm{i}u_t + \beta(t)u_{xx} + \chi(t)u\int_{-\infty}^{+\infty}|u|^2\mathrm{d}y = 0, \tag{2}$$

with the normalized complex field envelope $u(t, x, y)$, diffraction coefficient $\beta(t)$ and nonlinear coefficient $\chi(t)$. Here the subscripts denote the derivation to the corresponding variables. In this case, x-direction is localized, however, y-direction is nonlocal because the quantity at point y is related to other vicinal points. Equation (2) is a nonlinear differential–integral equation, and it is a variable-coefficient extension of the (2+1)-dimensional equation [30,31]. As reported in [30], Eq. (2) can be considered as the vector NLSE with infinitely many components. When β and χ are both constant, the Gram-type determinant solution and localized soliton interactions were studied [30]. More physical interpretation of Eq. (2) can also be found in Refs. [30,31].

2 Similarity reduction between nonlocal equation (2) and local equation (1)

Inserting the transformation

$$u(t, x, y) = \rho(y, t)U[X(x, t), T(t)] \times \exp[\mathrm{i}\phi(t, x, y)], \tag{3}$$

into Eq. (2), when function $U[X(x, t), T(t)]$ satisfies Eq. (1), we obtain the following set of equation

$$\rho_t + \beta\rho\phi_{xx} = 0,\ X_t + \beta X_x\phi_x = 0,$$
$$\phi_t + \beta\phi_x^2 = 0,\ T_t - 2\beta X_x^2 = 0,\ X_{xx} = 0, \tag{4}$$

$$\int_{-\infty}^{+\infty}\rho^2\mathrm{d}y = 2T_t/\chi. \tag{5}$$

After some algebra from Eqs. (4) and (5), we obtain the result: If $\beta(t)$ and $\chi(t)$ satisfy the relation

$$\chi(t) = -\frac{2}{w_0^2}\beta(t)\Pi(t), \tag{6}$$

then the amplitude, accumulated time, similarity variable and phase read

$$\rho(y, t) = A(y)\Omega(t),\ T(t) = \frac{\Omega(t)\Pi(t)}{w_0^2},$$
$$X(x, t) = \frac{x}{w(t)},$$
$$\phi(t, x, y) = -\frac{s_0\Omega(t)}{4}x^2 + \varphi(y), \tag{7}$$

and function $A(y)$ satisfies

$$\int_{-\infty}^{+\infty}|A(y)|^2\mathrm{d}y = 1, \tag{8}$$

with the width $w(t) = \frac{w_0}{\Omega(t)}$, the accumulated diffraction $\Pi(t) = \int_0^t\beta(\tau)\mathrm{d}\tau$, chirp function $\Omega(t) = [1 - s_0\Pi(t)]^{-1}$ and initial constants w_0, s_0 and free function $\varphi(y)$.

The normalization condition (8) for $A(y)$ hints that many types of function $A(y)$ can be selected. Function $A(y)$ can be the hyperbolic secant function as $A(y) = \mathrm{sech}(y)/\pi$. Moreover, function $A(y)$ can also be the Hermite–Gaussian function

$$A(y) = \frac{1}{\sqrt{n!2^n\sqrt{\pi}}}H_n(\omega y)e^{-\omega^2y^2/2}, \tag{9}$$

with the Hermite polynomial $H_n(\omega y)$ and nonnegative integer n.

Therefore, if $\beta(t)$ and $\chi(t)$ satisfy the relation (6), via the transformation (3) with (7), nonlocal equation (2) is reduced to the local equation (1).

3 Hierarchy of Peregrine solution

According to the modified Darboux transformation (DT) technique in Ref. [19] and choosing the plane-wave solution $u_0 = \exp(2\mathrm{i}T)$ as seed solution, from the one-to-one correspondence (3), we have the first-order rational solution (Peregrine solution)

$$u(t, x, y) = \frac{\Omega(t)}{\sqrt{n!2^n\sqrt{\pi}}}H_n(\omega y)e^{-\omega^2y^2/2}\left[-1 + \frac{G_1 + \mathrm{i}K_1}{D_1}\right] \times \exp\left\{\mathrm{i}[(2 - v^2)T_s + vX - \frac{s_0\Omega(t)}{4}x^2 + \varphi(y)]\right\}, \tag{10}$$

where $G_1 = 4$, $K_1 = 16T_s$, $D_1 = 1 + 4X_s^2 + 16T_s^2$ with $T_s = T - T_0$ and $X_s = X - vT_s$, and T and X are given in the expression (7).

Using solution (10) as the seed solution in DT technique, we obtain the second-order rational solution

$$u(t,x,y) = \frac{\Omega(t)}{\sqrt{n!2^n\sqrt{\pi}}} H_n(\omega y) e^{-\omega^2 y^2/2} \left[1 + \frac{G_2 + iK_2}{D_2}\right] \times \exp\left\{i[(2-v^2)T_s + vX - \frac{s_0\Omega(t)}{4}x^2 + \varphi(y)]\right\}, \quad (11)$$

where

$$G_2 = 36 - 15360T_s^4 - 3456T_s^2 - 192X_s^4 - 288X_s^2 - 4608T_s^2X_s^2,$$
$$K_2 = T_s(720 - 12288T_s^4 - 1536T_s^2 - 768X_s^4 + 1152X_s^2 - 6144T_s^2X_s^2),$$
$$D_2 = 9 + 4096T_s^6 + 6912T_s^4 + 1584T_s^2 + 64X_s^6 + 48X_s^4 + 108X_s^2 + 3072T_s^4X_s^2 + 768T_s^2X_s^4 - 1152T_s^2X_s^2$$

with $T_s = T - T_0$ and $X_s = X - vT_s$, and T and X are given in the expression (7).

Similarly, using solution (11) as the seed solution in DT technique, we obtain the third-order rational solution

$$u(t,x,y) = \frac{\Omega(t)}{\sqrt{n!2^n\sqrt{\pi}}} H_n(\omega y) e^{-\omega^2 y^2/2} \left[-1 + \frac{G_3 + iK_3}{D_3}\right] \times \exp\left\{i[(2-v^2)T_s + vX - \frac{s_0\Omega(t)}{4}x^2 + \varphi(y)]\right\}, \quad (12)$$

where $G_3 = 24576\,{X_s}^{10} + \left(92160 + 1474560\,{T_s}^2\right){X_s}^8 + (-1474560\,{T_s}^2 + 322560 + 19660800\,{T_s}^4){X_s}^6 + (-172800 + 2764800\,{T_s}^2 - 14745600\,{T_s}^4 + 110100480\,{T_s}^6){X_s}^4 + (-64800 - 20736000\,{T_s}^2 + 165888000\,{T_s}^4 + 165150720\,{T_s}^6 + 283115520\,{T_s}^8){X_s}^2 + 276824064\,{T_s}^{10} + 778567680\,{T_s}^8 + 215285760\,{T_s}^6 - 47001600\,{T_s}^4 - 777600\,{T_s}^2 + 16200$, $K_3 = 98304\,{X_s}^{10}T_s + \left(-368640\,T_s + 1966080\,{T_s}^3\right){X_s}^8 + (-921600\,T_s - 13762560\,{T_s}^3 + 15728640\,{T_s}^5){X_s}^6 + (-2073600\,T_s - 11059200\,{T_s}^3 - 82575360\,{T_s}^5 + 62914560\,{T_s}^7){X_s}^4 + (1814400\,T_s - 38707200\,{T_s}^3 + 168099840{T_s}^5 - 94371840\,{T_s}^7 + 125829120\,{T_s}^9){X_s}^2 + 100663296\,{T_s}^{11} + 157286400\,{T_s}^9 - 342097920\,{T_s}^7 - 236666880\,{T_s}^5 - 3801600\,{T_s}^3 + 453600\,T_s$, $D_3 = 4096\,{X_s}^{12} + (6144 + 98304\,{T_s}^2){X_s}^{10} + (34560 - 368640\,{T_s}^2 + 983040\,{T_s}^4){X_s}^8 + (149760 + 552960\,{T_s}^2 - 2949120\,{T_s}^4 + 5242880\,{T_s}^6){X_s}^6 + (54000 + 3456000\,{T_s}^2 - 5529600\,{T_s}^4 + 3932160\,{T_s}^6 + 15728640\,{T_s}^8){X_s}^4 + (48600 - 2332800\,{T_s}^2 + 80179200\,{T_s}^4 + 221184000\,{T_s}^6 + 70778880\,{T_s}^8 + 25165824\,{T_s}^{10}){X_s}^2 + 16777216\,{T_s}^{12} + 132120576\,{T_s}^{10} + 244776960\,{T_s}^8 + 62668800\,{T_s}^6 + 36806400\,{T_s}^4 + 1490400\,{T_s}^2 + 2025$ with $T_s = T - T_0$ and $X_s = X - vT_s$, and T and X are given in the expression (7).

Therefore, along this procedure, for any m-order, we can write the solution of Eq. (2) as follows

$$u(t,x,y) = \frac{\Omega(t)}{\sqrt{n!2^n\sqrt{\pi}}} H_n(\omega y) e^{-\omega^2 y^2/2} \times \left[(-1)^m + \frac{G_m + iK_m}{D_m}\right] \times \exp\left\{i[(2-v^2)T_s + vX - \frac{s_0\Omega(t)}{4}x^2 + \varphi(y)]\right\}, \quad (13)$$

where G_m, K_m and D_m are polynomials in the two variables T and X. For the limit of length, we do not list these expressions here.

4 Hierarchy of breather solution

According to the modified DT technique in Ref. [22] and choosing the plane-wave solution $u_0 = \exp(2iT)$ as seed solution, from the one-to-one correspondence (3), we derive the first-order breather solution

$$u(t,x,y) = \frac{\Omega(t)}{\sqrt{n!2^n\sqrt{\pi}}} H_n(\omega y) e^{-\omega^2 y^2/2} \times \left[-1 + \frac{L_1 + iM_1}{N_1}\right] \times \exp\left\{i[(2-v^2)T_s + vX - \frac{s_0\Omega(t)}{4}x^2 + \varphi(y)]\right\}, \quad (14)$$

where $L_1 = 2\kappa_1^2 \cosh\delta_1(T - T_1)$, $M_1 = 4\kappa_1\nu_1 \sinh\delta_1(T - T_1)$, $N_1 = 4[\cosh\delta_1(T - T_1) - \nu_1\cos\kappa_1(X - X_1)]$ with $\nu_1 = \mathrm{Im}(\lambda_1)$ and $\delta_1 = \nu_1\kappa_1$. Here T and X are given in the expression (7). When $0 < \nu_1 < 1$, this solution (14) describe breather, and when $\nu_1 > 1$ (κ_1 is imaginary), this solution (14) describes KM soliton. Specifically, if $\nu_1 \to 1$, this solution (14) can degenerate into the first-order rational solution (11) via the l'Hôpital's rule.

When we consider the second-order solution, two independent frequencies of modulation, κ_1 and κ_2, are combined in the solution via the next step of the DT. Along the procedure in Ref. [22], we derive the second-order breather solution

$$u(t,x,y) = \frac{\Omega(t)}{\sqrt{n!2^n\sqrt{\pi}}} H_n(\omega y) e^{-\omega^2 y^2/2} \times \left[1 + \frac{L_2 + \mathrm{i}M_2}{N_2}\right] \times \exp\left\{\mathrm{i}[(2-v^2)T_s + vX - \frac{s_0\Omega(t)}{4}x^2 + \varphi(y)]\right\}, \quad (15)$$

where $L_2 = -\kappa_{12}[\kappa_1^2\delta_2\cosh(\delta_1 T_{s1})\cos(\kappa_2 X_{s2})/\kappa_2 - \kappa_2^2\delta_1\cosh(\delta_2 T_{s2})\cos(\kappa_1 X_{s1})/\kappa_1 - \kappa_{12}\cosh(\delta_1 T_{s1})\cosh(\delta_2 T_{s2})]$, $M_2 = -2\kappa_{12}[\delta_1\delta_2\sinh(\delta_1 T_{s1})\cos(\kappa_2 X_{s2})/\kappa_2 - \delta_2\delta_1\sinh(\delta_2 T_{s2})\cos(\kappa_1 X_{s1})/\kappa_1 - \delta_1\sinh(\delta_1 T_{s1})\cosh(\delta_2 T_{s2}) + \delta_2\cosh(\delta_1 T_{s1})\sinh(\delta_2 T_{s2})]$, $N_2 = 2(\kappa_1^2+\kappa_2^2)\delta_1\delta_2\cos(\kappa_1 X_{s1})\cos(\kappa_2 X_{s2})/(\kappa_1\kappa_2) - (2\kappa_1^2 - \kappa_1^2\kappa_2^2 + 2\kappa_2^2)\cosh(\delta_1 T_{s1})\cosh(\delta_2 T_{s2}) + 4\delta_1\delta_2[\sin(\kappa_1 X_{s1})\sin(\kappa_2 X_{s2}) + \sinh(\delta_1 T_{s1})\sinh(\delta_2 T_{s2})] - 2\kappa_{12}[\delta_1\cos(\kappa_1 X_{s1})\cosh(\delta_2 T_{s2})/\kappa_1 - \delta_2\cos(\kappa_2 X_{s2})\cosh(\delta_1 T_{s1})/\kappa_2]$ with $T_{sj} = 2(T - T_j)$, $X_{sj} = X - X_j$, $\delta_j = \kappa_j\sqrt{4-\kappa_j^2}/2$, $\kappa_{12} = \kappa_1^2 - \kappa_2^2$, $\kappa_j = 2\sqrt{1+\lambda_j^2}$, $j = 1, 2$. Here κ is the modulation frequency, T_j and X_j determine the center of solution in t-x coordinates, and T and X are given in the expression (7).

When the values of $\mathrm{Im}(\lambda_1)$ and $\mathrm{Im}(\lambda_2)$ are both between 0 and 1, this solution (15) describes two breathers. When the values of $\mathrm{Im}(\lambda_1)$ and $\mathrm{Im}(\lambda_2)$ are both bigger than 1, this solution (15) describes two Kuznetsov-Ma solitons. For the values of $\mathrm{Im}(\lambda_1)$ and $\mathrm{Im}(\lambda_2)$, if one of them is bigger than 1, and another is between 0 and 1, a breather and a Kuznetsov-Ma soliton can be constructed together.

Especially, if $\kappa_1 \neq 0$ and $\kappa_2 \to 0$, solution (15) describes a breather or a Kuznetsov-Ma soliton with a Peregrine solution. In this case, expressions of L_2, M_2 and N_2 in solution (15) has the form

$$L_2 = \kappa\{\kappa[\kappa^2(4T_{s2}^2 + 4X_{s2}^2 + 1) - 8] \times \cosh(\delta T_{s1}) + 8\delta\cos(\kappa X_{s1})\}/8,$$
$$M_2 = \kappa\{8T_{s2}[\delta\cos(\kappa X_{s1}) - \kappa\cosh(\delta T_{s1})] + \delta\kappa(4T_{s2}^2 + 4X_{s2}^2 + 1)\sinh(\delta T_{s1})\}/4,$$
$$N_2 = -\{\delta[\kappa^2(4T_{s2}^2 + 4X_{s2}^2 + 1) - 16] \times \cos(\kappa X_{s1}) + \kappa([\kappa^2(4T_{s2}^2 + 4X_{s2}^2 - 3) + 16] \times \cosh(\delta T_{s1}) - 16\delta[T_{s2}\sinh(\delta T_{s1}) + X_{s2}\sin(\kappa X_{s1})])\}/(4\kappa) \quad (16)$$

with $T_{sj} = 2(T - T_j)$, $X_{sj} = X - X_j$, $\delta = \kappa\sqrt{4-\kappa^2}/2$, $\kappa = 2\sqrt{1+\lambda_1^2}$, $j = 1, 2$. When $0 < \mathrm{Im}(\lambda_1) < 1$ and $\mathrm{Im}(\lambda_1) > 1$ in solution (16), we can obtain the Peregrine solution combined by a breather and Kuznetsov-Ma soliton, respectively.

Similarly, along the procedure in Ref. [22], we derive m-order solution

$$u(t,x,y) = \frac{\Omega(t)}{\sqrt{n!2^n\sqrt{\pi}}} H_n(\omega y) e^{-\omega^2 y^2/2} \times \left[(-1)^m + \frac{L_m + \mathrm{i}M_m}{N_m}\right] \times \exp\left\{\mathrm{i}[(2-v^2)T_s + vX - \frac{s_0\Omega(t)}{4}x^2 + \varphi(y)]\right\}, \quad (17)$$

where L_m, M_m and N_m are polynomials in the two variables T and X. For the limit of length, we do not list these expressions here.

5 Controllable behaviors of localized structures

The controllable behaviors of localized structures are studied in the following soliton control system [32,33]

$$\beta(t) = \beta_0 \exp(-\sigma t), \quad (18)$$

which is the exponentially modulated control system. Parameter β_0 describes the initial diffraction. This system is a typical diffraction decreasing system (DDS) for $\sigma > 0$. Moreover, if $\sigma = 0$, Eq.(18) is a constant diffraction system.

At first, we reconsider the excitation of Peregrine solution (10) in the framework of the focusing NLSE (1). As reported in Ref. [19], Peregrine solution reaches its maximum at center point ($X_0 = 0$, T_0). Along T-axis, Peregrine solution is excited from a continuous-wave background (emerging at $T \approx T_0$) and disappears soon.

Note that the accumulated time T and similarity variable X are not real time t and real spatial variable x in our study, respectively. From the expression

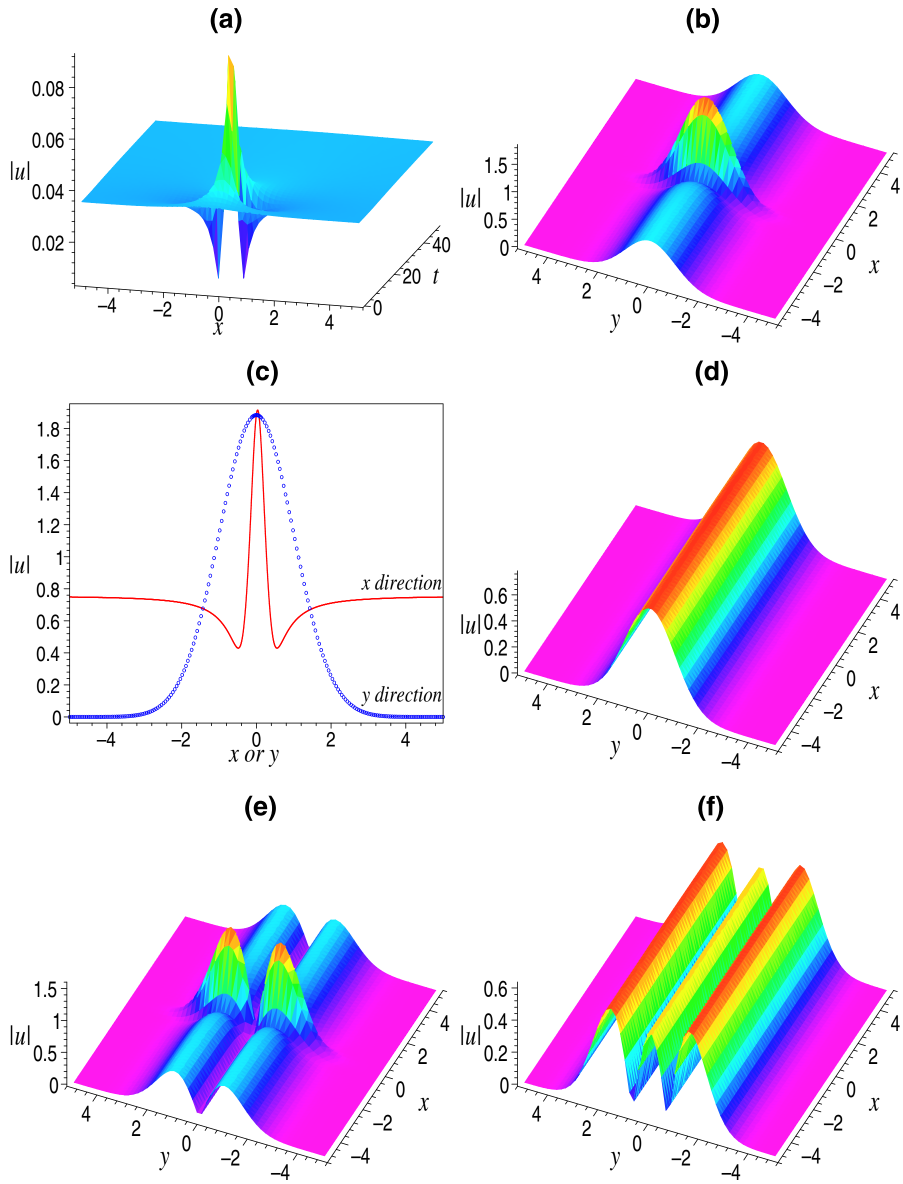

Fig. 1 Complete excitation of Peregrine solution in DDS at **a** x-t plane with $y = 3$ and **b**–**f** x-y space with **b, c** $n = 0, t = 8$, **d** $n = 0, t = 100$, **e** $n = 1, t = 8$, and **f** $n = 2, t = 100$. Parameters are chosen as $w_0 = 0.5, \beta_0 = 0.1, \sigma = 0.05, s_0 = 0.02, v = 0.2, T_0 = 5, \omega = 1$

$T(t) = \frac{\Omega(t)\Pi(t)}{w_0^2}$ in Eq. (7), we know that the value of $T(t)$ is not free, and it is limited to a certain range. In the DDS, $T(t) = \frac{\beta_0[1-\exp(-\sigma t)]}{w_0^2\{\sigma - s_0\beta_0[1-\exp(-\sigma t)]\}}$, which indicates that $T(t) \to T_m \equiv \frac{\beta_0}{w_0^2[\sigma - s_0\beta_0]}$ as real time $t \to \infty$.

Therefore, the relation between T_0 and T_m is crucial to determine the degree of excitation. As reported in our previous study [24,25,27], if $T_m > T_0$, Peregrine solution is completely and quickly excited; if $T_m = T_0$, Peregrine solution is excited to peak and maintain this shape a long time; if $T_m < T_0$, Peregrine solution is only excited to initial shape. Note that here we discuss the control for the excitation of two-dimensional localized Peregrine solution, which is hardly studied to the best of our knowledge, and different from two-dimensional line rogue waves reported in [27–29].

Figure 1 shows the complete excitation of Peregrine solution with $T_m = 16.67 > T_0 = 5$. Figure 1a exhibits the complete excitation of Peregrine solution at the range of $5 < t < 11$ in the x-t plane. In x-y space, the combined structure is made up of the Hermite–Gaussian structure in y-component and Peregrine solu-

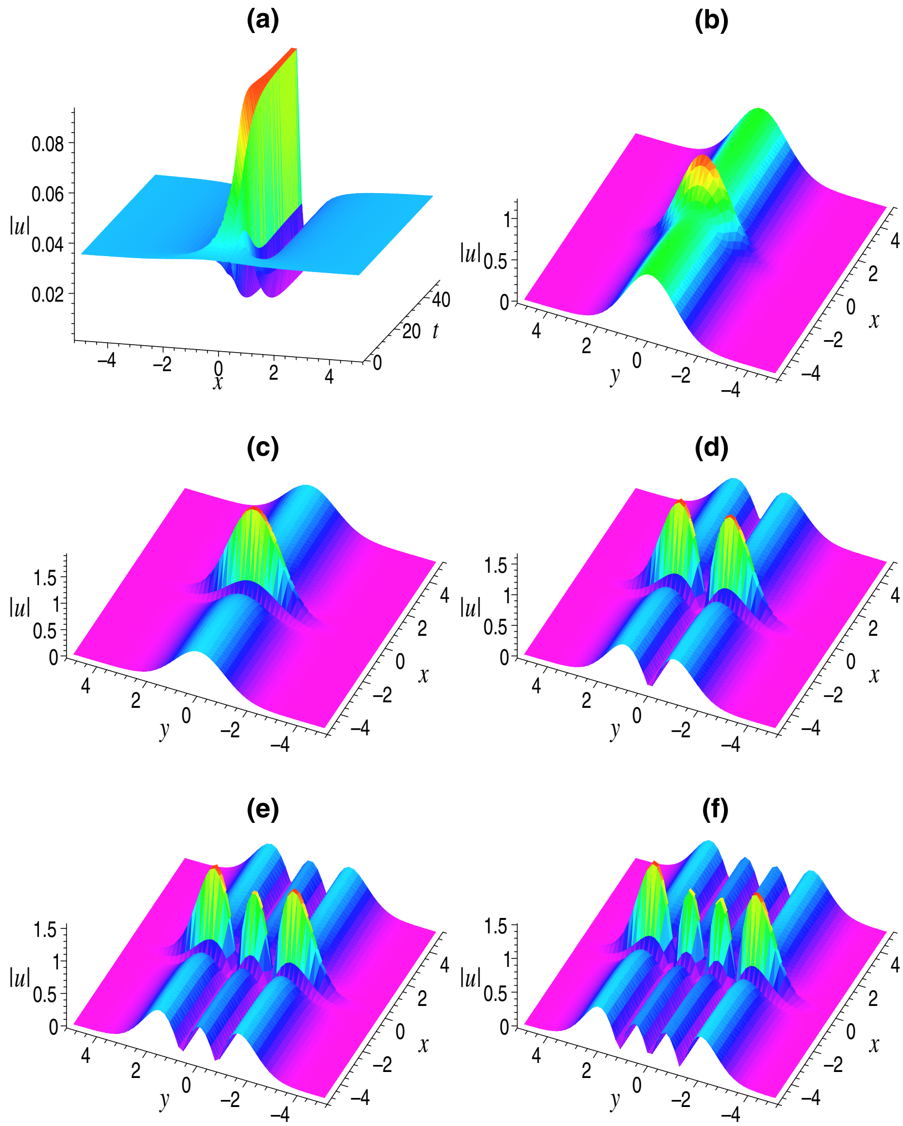

Fig. 2 Peak excitation of Peregrine solution in DDS at **a** x-t plane with $y = 3$ and **b–f** x-y space with **b** $n = 0, t = 10$, **c** $n = 0, t = 100$, **d** $n = 1, t = 10$, **e** $n = 2, t = 100$, and **f** $n = 3, t = 100$. Parameters are chosen as $w_0 = 0.5, \beta_0 = 0.1, \sigma = 0.162, s_0 = 0.02, v = 0.2, T_0 = 5, \omega = 1$

tion. During the stage of complete excitation, the combined structure in x-y space appear a localized structure at the range of $-0.5 < x < 0.5$ in Fig. 1b when $n = 0$. Corresponding to Fig. 1b, the detailed structures in x-direction (when $y = 0$) and y-direction (when $x = 0$) are shown in Fig. 1c. When $t > 11$, there is a constant plane in the x-t plane, and thus only the Gaussian structure is shown in x-y space in Fig. 1d. For $n = 1$, when $t = 8$, two localized wave packets [like structures in Fig. 1c] appear in the x-t plane in Fig. 1e. When $t = 100$, there is a constant plane in the x-t plane, and thus only the Hermite–Gaussian structure is shown in x-y space. For other values of n, if $t > 11$, there are only the Hermite–Gaussian structures in x-y space. Figure 1f is another example of the Hermite–Gaussian structure in x-y space when $n = 2$.

If $T_m = T_0 = 5$, the peak excitation of Peregrine solution can maintain a long time with a self-similar propagating behavior in Fig. 2a, where its amplitude and width self-similarly change after a short propagation time from the initial condition. Corresponding to the initial stage of excitation in Fig. 2a, a wave packet is embedded in a line Gaussian structure in x-y space in Fig. 2b at $t = 10$ when $n = 0$. Corresponding to the peak stage of excitation in Fig. 2a, the combined structure in x-y space appear localized structure [like

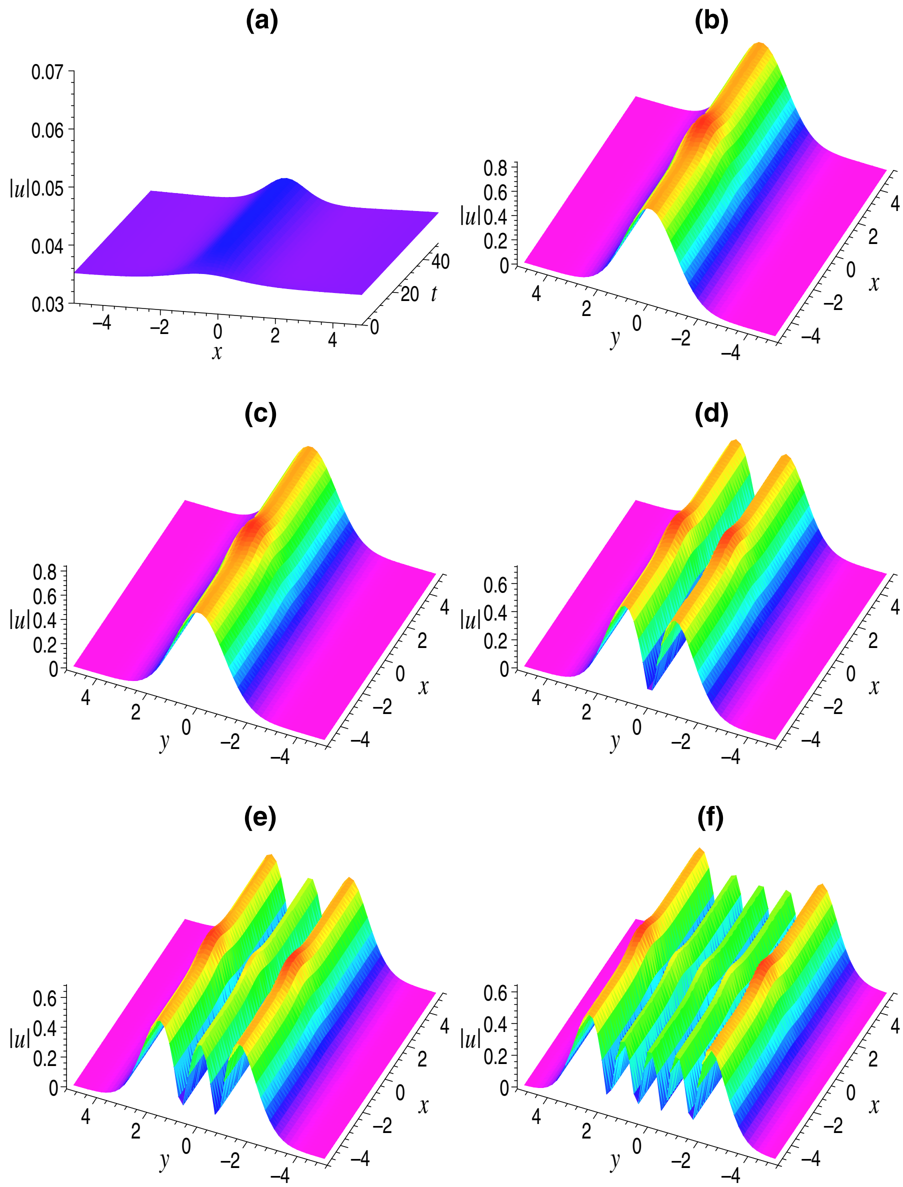

Fig. 3 Initial excitation of Peregrine solution in DDS at **a** x-t plane with $y = 3$ and **b–f** $x - y$ space with **b** $n = 0, t = 10$, **c** $n = 0, t = 100$, **d** $n = 1, t = 10$, **e** $n = 2, t = 100$, and **f** $n = 4, t = 100$. Parameters are chosen as $w_0 = 0.5, \beta_0 = 0.1, \sigma = 0.4, s_0 = 0.02, v = 0.2, T_0 = 5, \omega = 1$

structure in Fig. 1c] at the range of $-0.5 < x < 0.5$ in Fig. 2c when $t = 100$. Similarly, for other values of n, if $t > 11$, there are all localized structures [like structures in Fig. 1c] in x-y space, and the number of localized structures is decided by $n + 1$ for n-th order of Hermite polynomial. Figure 2d–f demonstrates these localized structures [like structures in Fig. 1c] for different n.

If $T_m = 2.01 < T_0 = 5$, the excitation of Peregrine solution is restrained and only excited to initial shape in Fig. 3a because the threshold of exciting Peregrine solution is never reached. This structure looks like a bright optical similariton and separated bright similariton pairs [34] with very small amplitudes propagating stably on a non-zero background. In x-y space, no localized structures appear. From Fig. 3b ($t = 10$) to Fig. 3c ($t = 100$), only a small packet is superimposed on a line Gaussian structure when $n = 0$. For other values of n, only small packets are also superimposed on the line Hermite–Gaussian structures. Some examples are shown in Fig. 3d–f.

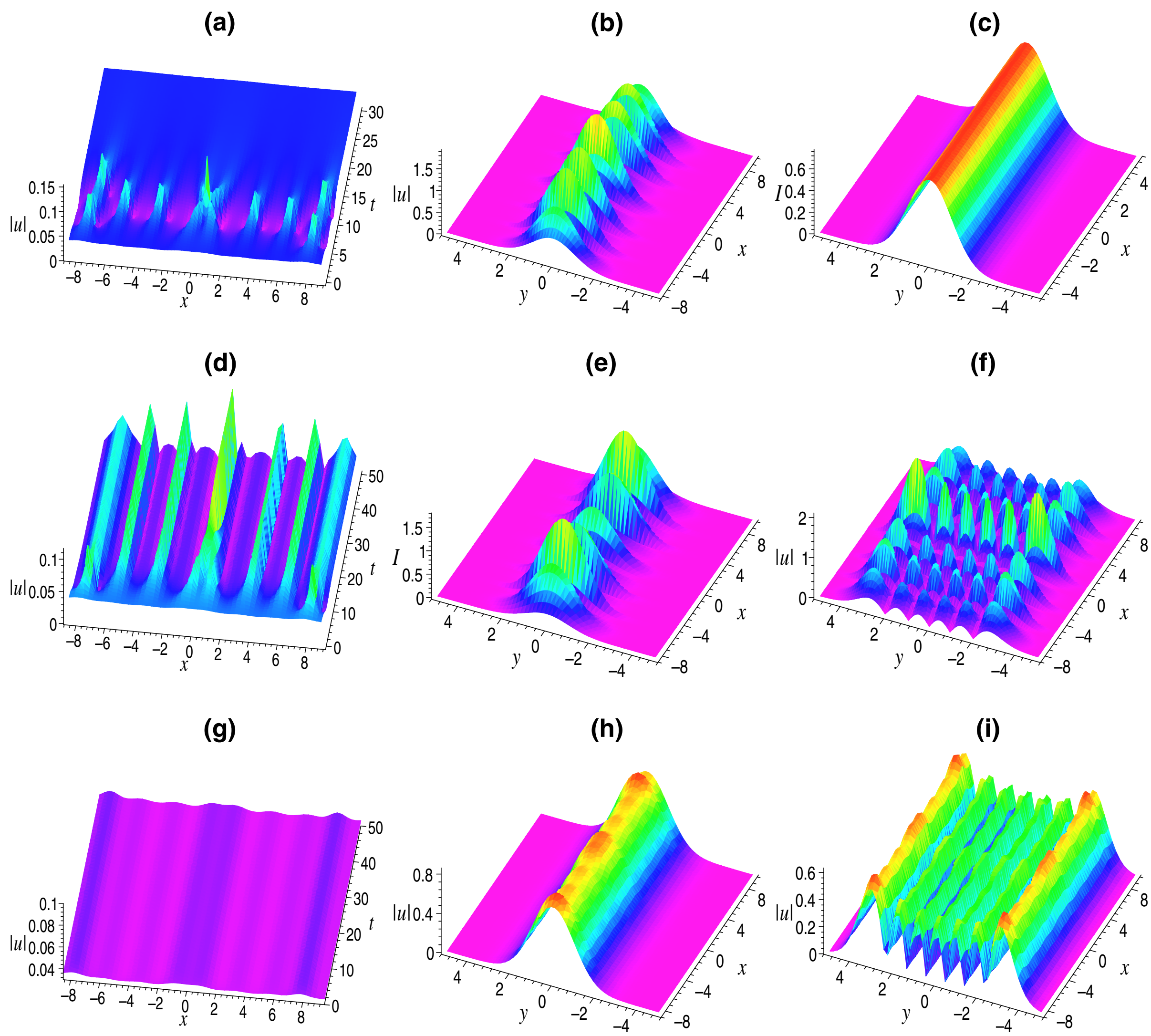

Fig. 4 Complete excitation of superposed breather in DDS at **a** x-t plane with $y = 3$ and x-y space with **b** $n = 0, t = 7$, **c** $n = 0, t = 100$; peak excitation of superposed breather in DDS at **d** x-t plane with $y = 3$ and x-y space with **e** $n = 0, t = 100$, **f** $n = 5, t = 100$; initial excitation of superposed breather in DDS at **g** x-t plane with $y = 3$ and x-y space with **h** $n = 0, t = 100$, **i** $n = 6, t = 100$. Parameters are chosen as $\kappa_1 = 0.4, \kappa_2 = 1.4, w_0 = 0.5, \beta_0 = 0.1, s_0 = 0.02, v = 0.2, T_1 = T_2 = 5, \omega = 1$ with **a–c** $\sigma = 0.05$, **d–f** $\sigma = 0.162$ and **g–i** $\sigma = 0.4$

For other order rational solutions, when $T_m > T_0$, $T_m = T_0$ and $T_m < T_0$, complete excitation, peak excitation and initial excitation will happen. These cases are similar to Peregrine solution in Figs. 1–3. For the limit of length, we omit the related plots.

In the following, we consider the control of the excitation of superposed breather. Solution (15) can describe two arrays of separated breathers. Each breathers are composed of Peregrine solution-like structures. In each arrays, the numbers of Peregrine solution-like structures are decided by the ratio of κ_1 and κ_2. When two arrays of separated breathers share the same origin, we can construct superposed breathers. Similarly to these excitations of Peregrine solution in Figs. 1–3, when $T_m > T_1 = T_2$, $T_m = T_1 = T_2$ and $T_m < T_1 = T_2$, complete excitation, peak excitation and initial excitation of superposed breather will occur.

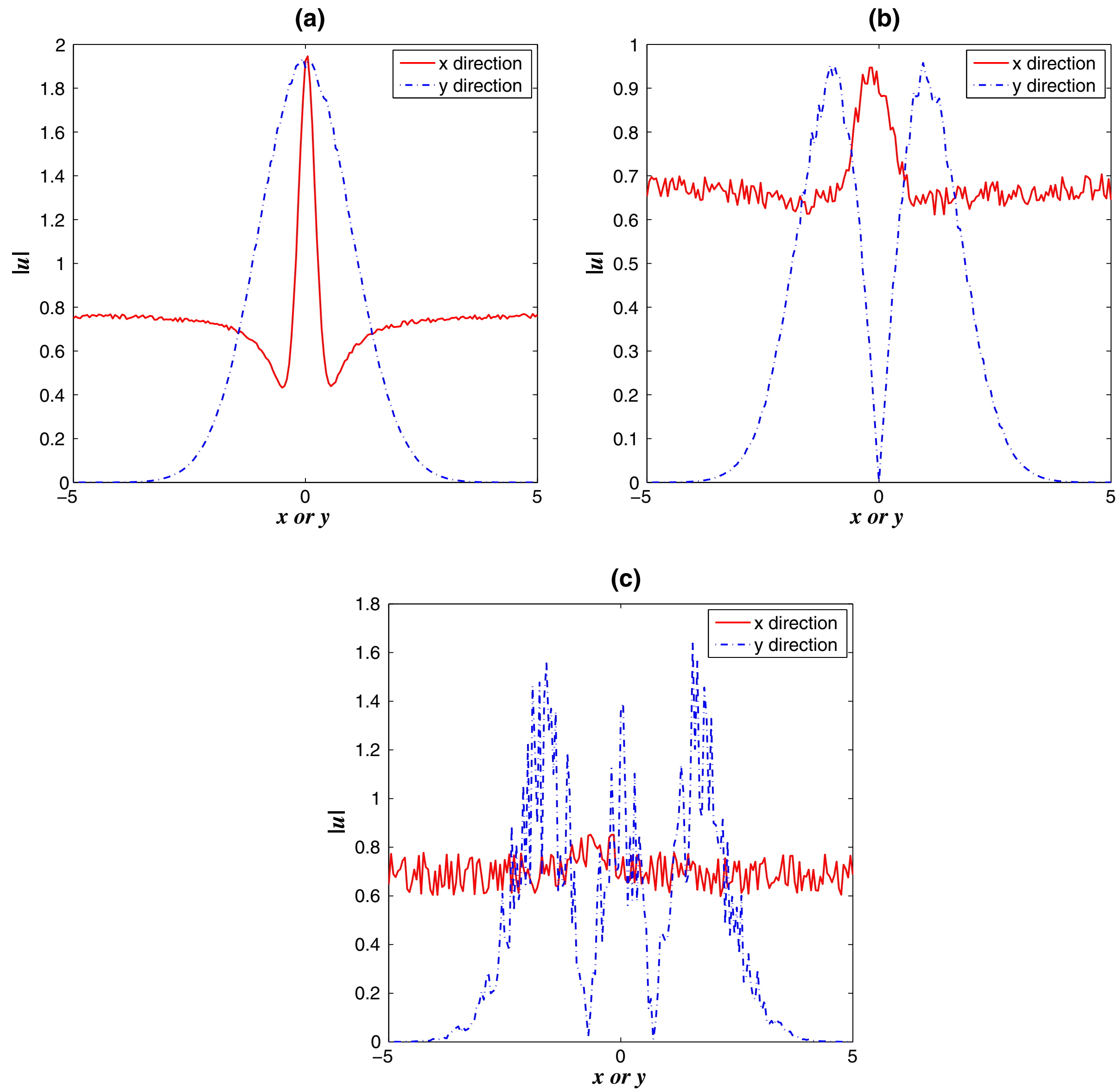

Fig. 5 Numerical rerun of Peregrine solution (10) in Figs. 1c, 2d and 3e at time $t = 100$. An added 5% white noise is added to the initial values. The parameters are the same as those in the corresponding analytical plots

Here we choose $\kappa_1 = 0.2$ and $\kappa_2 = 1.4$, namely, the number of Peregrine solution-like structures in two array is $1 : 7$. When they share the same origin, two Peregrine solution-like structures with the same value of x form a parallel Peregrine solution-like pair, and three Peregrine solution-like structures triangularly laying out become a second-order rational solution.

If T_m is remarkably bigger than $T_1 = T_2$, the full superposed breather is excited completely. Figure 4a shows the complete excitation at the range of $0 < t < 17$ in the x-t plane. In x-y space, the combined structure is made up of the Hermite–Gaussian structure in y-direction and breather in x-direction. During the stage of complete excitation, in x-y space, the combined structure appears a breather in x-direction with Gaussian structures in y-direction in Fig. 4b when $n = 0$. When $t > 17$, there is a constant plane in the x-t plane, and thus only the Gaussian structure is shown in x-y space in Fig. 4c. For other values of n, $(n + 1)$-arrays of breathers appear at the range of $0 < t < 17$, and the Hermite–Gaussian structure appears at $t > 17$ in x-y space.

If $T_m = T_1 = T_2$, in x-t plane, the peak excitation of superposed breather can maintain a long time with self-similar propagating behaviors (see Fig. 4d). The amplitude and width of sustained breather self-similarly change after a short propagation time from the initial condition. Corresponding to the initial stage of excitation in Fig. 4d, the combined structure in x-y space appears a breather in Fig. 4e when $t = 100$. Similarly, for other values of n, if $t > 11$, there are $(n + 1)$-arrays of breathers in x-y space. For example, Fig. 4f displays six arrays of breathers in x-y space when $n = 5$.

If $T_m < T_1 = T_2$, the threshold of exciting superposed breather is never reached, its excitation is restrained an d only initial part is excited in the x-t plane (see Fig. 4g), which looks like a periodic wave with very small amplitudes propagating stably with the time. In x-y space, only some small packets are superimposed on the line Hermite–Gaussian structures. Figure 4h, demonstrate two examples when $n = 0$ and $n = 6$, respectively.

At last, we discuss the stability of these Peregrine solutions with different controllable excitations. We study analytical solutions evolving with time when they are disturbed from their analytically given forms. We perform the direct numerical simulation (the split-step Fourier technique) with initial white noise for Eq. (2) with initial fields coming from solution (10) in some cases. Figure 5 displays the numerical rerun of Peregrine solution (10) in Figs. 1c, 2d and 3e at time $t = 100$. From Fig. 5a, one can find that Peregrine solution with complete excitation for $n = 1$ stably evolves with time in both x and y directions, and the white noise hardly influences the evolution of Peregrine solution. In Fig. 5b, the white noise has a stronger influence on Peregrine solution with peak excitation for $n = 2$, especially two sides of Peregrine solution in x-direction. From Fig. 5c, Peregrine solution with initial excitation for $n = 3$ is unstable and broken down the initial shape after evolving time $t = 100$, and at last turns into noise especially for its shape in x-direction. Compared these Peregrine solutions in Fig. 5a–c, the stability attenuates with the add of n.

6 Conclusions

In conclusion, we obtain hierarchies of Peregrine solution and breather solution excited in a (2+1)-dimensional variable-coefficient NLSE with partial nonlocality. Based on these solutions, we study the control of the excitation of Peregrine solution and breather solution in different planes. If $T_m > T_0 (\text{or} T_1 = T_2)$, Peregrine solution or breather solution is completely and quickly excited; if $T_m = T_0 (\text{or} T_1 = T_2)$, Peregrine solution or breather solution is excited to peak and maintain this shape a long time; if $T_m < T_0 (\text{or} T_1 = T_2)$, Peregrine solution or breather solution is only excited to initial shape. In particular, we report firstly the localized Peregrine solution and breather solution in two-dimensional space. Numerical rerun for analytical solution indicates that the stability of Peregrine solution attenuates with the add of n. It is expected that our analysis and results may give new insight into higher-dimensional localized rogue waves in nonlocal media.

Acknowledgements This work was supported by the Zhejiang Provincial Natural Science Foundation of China (Grant No. LY17F050011), the National Natural Science Foundation of China (Grant No. 11375007). Dr. Chao-Qing Dai is also sponsored by the Foundation of New Century "151 Talent Engineering" of Zhejiang Province of China and Youth Top-notch Talent Development and Training Program of Zhejiang A & F University.

References

1. Zhou, Q., Yu, H., Xiong, X.: Optical solitons in media with time-modulated nonlinearities and spatiotemporal dispersion. Nonlinear Dyn. **80**, 983–987 (2015)
2. Xu, S.L., Zhou, G.P., Petrović, N.Z., Belić, M.R.: Nonautonomous vector matter waves in twocomponent Bose-Einstein condensates with combined time-dependent harmonic-lattice potential. J. Opt. **17**, 105605 (2015)
3. Dai, C.Q., Fan, Y., Zhou, G.Q., Zheng, J., Cheng, L.: Vector spatiotemporal localized structures in (3 + 1)-dimensional strongly nonlocal nonlinear media. Nonlinear Dyn. **86**, 999–1005 (2016)
4. Chen, Y.X., Jiang, Y.F., Xu, Z.X., Xu, F.Q.: Nonlinear tunnelling effect of combined Kuznetsov–Ma soliton in (3+1)-dimensional PT-symmetric inhomogeneous nonlinear couplers with gain and loss. Nonlinear Dyn. **82**, 589–597 (2015)
5. Wang, Y.Y., Dai, C.Q.: Caution with respect to "new" variable separation solutions and their corresponding localized structures. Appl. Math. Model. **40**, 3475–3482 (2016)

6. Dai, C.Q., Wang, Y.Y., Biswas, A.: Dynamics of dispersive long waves in fluids. Ocean Eng. **81**, 77–88 (2014)
7. Xu, S.L., Petrovic, N., Belic, M.R.: Exact solutions of the (3+1)-dimensional cubic-quintic nonlinear Schrödinger equation with variable coefficients. Nonlinear Dyn. **81**, 574–579 (2016)
8. Xu, S.L., Petrović, N.Z., Belić, M.R.: Exact solutions of the (2+1)-dimensional quintic nonlinear Schrodinger equation with variable coefficients. Nonlinear Dyn. **80**, 583–589 (2015)
9. Xu, S.L., Cheng, J.X., Belić, M.R., Hu, Z.L., Zhao, Y.: Dynamics of nonlinear waves in two-dimensional cubic-quintic nonlinear Schrodinger equation with spatially modulated nonlinearities and potentials. Opt. Express **24**, 10066 (2016)
10. Solli, D.R., Ropers, C., Koonath, P., Jalali, B.: Optical rogue waves. Nature **450**, 1054–1057 (2007)
11. Li, J.T., Zhang, X.T., Meng, M., Liu, Q.T., Wang, Y.Y., Dai, C.Q.: Control and management of the combined Peregrine soliton and Akhmediev breathers in PT-symmetric coupled waveguides. Nonlinear Dyn. **84**, 473–479 (2016)
12. Kharif, C., Pelinovsky, E., Slunyaev, A.: Rogue Waves in the Ocean. Springer, Heidelberg (2009)
13. Bludov Yu, V., Konotop, V.V., Akhmediev, N.: Matter rogue waves. Phys. Rev. A **80**, 033610 (2009)
14. Akhmediev, N., Ankiewicz, A., Taki, M.: Waves that appear from nowhere and disappear without a trace. Phys. Lett. A **373**, 675–678 (2009)
15. Broad, W. J.: Rogue giants at sea. The New York Times, July 11 (2006)
16. Osborne, A.R.: Nonlinear Ocean Waves. Academic Press, New York (2009)
17. Dudley, J.M., Genty, G., Eggleton, B.J.: Harnessing and control of optical rogue waves in supercontinuum generation. Opt. Express **16**, 3644–3651 (2008)
18. Dudley, J.M., Genty, G., Dias, F., Kibler, B., Akhmediev, N.: Modulation instability, Akhmediev Breathers and continuous wave supercontinuum generation. Opt. Express **17**, 21497–21508 (2009)
19. Akhmediev, N., Ankiewicz, A., Soto-Crespo, J.M.: Rogue waves and rational solutions of the nonlinear Schrödinger equation. Phys. Rev. E **80**, 026601 (2009)
20. Akhmediev, N., Soto-Crespo, J.M., Ankiewicz, A.: How to excite a rogue wave. Phys. Rev. A **80**, 043818 (2009)
21. Akhmediev, N., Soto-Crespo, J.M., Ankiewicz, A.: Extreme waves that appear from nowhere: on the nature of rogue waves. Phys. Lett. A **373**, 2137–2145 (2009)
22. Kedziora, D.J., Ankiewicz, A., Akhmediev, N.: Second-order nonlinear Schrodinger equation breather solutions in the degenerate and rogue wave limits. Phys. Rev. E **85**, 066601 (2012)
23. Serkin, V.N., Hasegawa, A., Belyaeva, T.L.: Nonautonomous solitons in external potentials. Phys. Rev. Lett. **98**, 074102 (2007)
24. Tian, Q., Yang, Q., Dai, C.Q., Zhang, J.F.: Controllable optical rogue waves: recurrence, annihilation and sustainment. Opt. Commun. **284**, 2222–2225 (2011)
25. Dai, C.Q., Zhou, G.Q., Zhang, J.F.: Controllable optical rogue waves in the femtosecond regime. Phys. Rev. E **85**, 016603 (2012)
26. Hu, W.C., Zhang, J.F., Zhao, B., Lou, J.H.: Transmission control of nonautonomous optical rogue waves in nonlinear optical media. Acta Phys. Sin. **62**, 024216 (2013)
27. Dai, C.Q., Wang, Y.Y., Zhou, G.Q.: The realization of controllable three dimensional rogue waves in nonlinear inhomogeneous system. Ann. Phys. **327**, 512–521 (2012)
28. Zhang, J.F., Lou, J.H.: Line optical rogue waves and transmission controlling in inhomogeneous nonlinear waveguides. Acta Opt. Sin. **33**, 0919001 (2013)
29. Dai, C.Q., Wang, Y.Y.: Superposed Akhmediev breather of the (3+1)-dimensional generalized nonlinear Schrödinger equation with external potentials. Ann. Phys. **341**, 142–152 (2014)
30. Maruno, K., Ohta, Y.: Localized solitons of a (2 +1)-dimensional nonlocal nonlinear Schrödinger equation. Phys. Lett. A **372**, 4446–4450 (2008)
31. Yan, Z.Y.: Rogon-like solutions excited in the two-dimensional nonlocal nonlinear Schrödinger equation. J. Math. Anal. Appl. **380**, 689–696 (2011)
32. Serkin, V.N., Belyaeva, T.L., Alexandrov, I.V., Melchor, G.M.: Novel topological quasi-soliton solutions for the nonlinear cubic-quintic Schrodinger equation model. Proc SPIE **4271**, 292–302 (2001)
33. Dai, C.Q., Wang, Y.Y., Wang, X.G.: Ultrashort self-similar solutions of the cubic-quintic nonlinear Schrodinger equation with distributed coefficients in the inhomogeneous fiber. J. Phys. A Math. Theor. **44**, 155203 (2011)
34. Dai, C.Q., Zhu, S.Q., Wang, L.L.: Exact spatial similaritons for the generalized (2+1)-dimensional nonlinear Schrodinger equation with distributed coefficients. Europhys. Lett. **92**, 24005 (2010)